

Chronic Prediction of Peripheral Artery Disease Progression to Kidney Disease Using a Multi-branch Hybrid Deep Neural Network

Nazia Sultana^{1*}, and Dr.P.K. Kumar²

^{1*}Research Scholar, Department of Computer Science & Engineering,
Visvesvaraya Technological University, Postgraduate Centre, Mysuru, Karnataka, India.
naziasultana@vtu.ac.in, <https://orcid.org/0009-0008-5104-6793>

²Assistant Professor, Department of Computer Science & Engineering,
Visvesvaraya Technological University, Postgraduate Centre, Mysuru, Karnataka, India.
kumar.pk@vtu.ac.in, <https://orcid.org/0000-0003-2786-7889>

Received: January 06, 2026; Revised: February 23, 2026; Accepted: March 27, 2026; Published: May 29, 2026

Abstract

Peripheral Artery Disease (PAD) and chronic kidney disease (CKD) are highly correlated conditions of the vascular and metabolic systems, which cause high rates of morbidity and mortality across the globe. The identification of the early development of PAD to CKD is still a clinically complicated issue with complicated multimodal patterns of data and a late onset of symptoms. The proposed study is a multi-branch hybrid deep neural network that combines Xception, VGG19, and Efficient Net to predict chronic progression of PAD to CKD based on multimodal medical images and clinical data (CT imaging and MIMIC-III EHR dataset). These complementary CNN models can be fused to learn features, which can be further used to predict and learn features, and thus provide strong representation learning. Experimental analysis shows that the proposed model attains an accuracy of 99.55, precision of 99.65, recall of 99.50, and F1-score of 99.60, which is higher than individual CNN architectures and traditional deep learning models in various feature-selection strategies and validation splits. The framework is also computationally efficient; thus, it can be deployed in resource-constrained healthcare settings. Along with the high predictive accuracy of PAD to CKD development, the suggested multi-branch hybrid deep neural network (DNN) model is also concerned with the safe treatment of patient data. Secure data transmission protocols, encryption, and access control mechanisms are employed to guarantee the confidentiality and integrity of sensitive medical information. These security measures will comply with healthcare data protection requirements and adhere to privacy laws such as HIPAA. These findings substantiate the power of hybrid feature fusion and multi-branch learning in predicting early disease progression as a reliable and scalable AI-aided decision-support system to support clinical risk stratification and patient management.

Keywords: Chronic Kidney Disease (CKD), Peripheral Artery Disease (PAD), Multi-Branch Deep Learning, Hybrid CNN, Healthcare Data Security, Medical Imaging AI, Disease Progression Prediction.

1 Introduction

Both Peripheral Artery Disease (PAD) and chronic kidney disease (CKD) are common conditions that go hand in hand as both share some risk factors, including hypertension, diabetes, smoking, and high cholesterol (Levin et al., 2007). PAD is a condition where the arteries are narrowed, which lowers the blood flow to the lower limbs, resulting in symptoms such as pain and cramping of the legs. By comparison, CKD is characterized by the progressive loss of kidney function, and one of the determining factors of the condition is a decrease in blood flow to the kidneys (Koelzer et al., 2016). These are not only worsened by atherosclerosis, in which fatty deposits constrict blood vessels, reducing the amount of oxygen and nutrients reaching vital organs. In CKD patients with PAD, the condition speeds the progression of kidney damage as it impairs blood flow to the kidneys, further disturbing renal functioning, which adds to a vicious cycle of worsening health (Han et al., 2019). Although deep learning has shown promise in predicting the progression of PAD to CKD, the aspect of data security among the patient's data cannot be overlooked. With the increase in the use of AI models in the operation of healthcare systems, there is a need to ensure that sensitive information such as private medical records cannot be interfered with (Khalid et al., 2023). There must be data protection during transfer, encryption of the patient's data, and limiting access to health records. These actions should be taken care of in the AI models.

The two conditions are mutually dependent, making it hard to diagnose and treat. The progression of PAD leads to reduced kidney perfusion while CKD exacerbates the progression of PAD through fluid retention and electrolyte imbalance, leading to vascular calcification. These effects increase the rate of atherosclerosis, risking heart attacks, strokes, and kidney failure (Chen et al., 2025). Early detection of these conditions may be difficult due to the symptoms of PAD, where symptoms are absent in the early stages while CKD is mostly diagnosed when the condition is already in its advanced stages. Tests such as the Ankle-Brachial Index test for PAD and blood tests for CKD are key diagnostic tools (Gharaibeh et al., 2022).

The treatment of both PAD and CKD is complicated as it depends upon a number of factors including changes in lifestyle, risk factor modification, and in serious cases surgery (angioplasty or dialysis). However, the presence of these diseases together reduces the efficiency of the treatment methods applied on these patients. Therefore, in order to provide better results to the patient, it becomes essential to make a proper diagnostic and treatment plan. Moreover, an early diagnosis along with technological advancements like artificial intelligence and machine learning will contribute significantly towards improving the accuracy of diagnosis.

Table 1: GFR values determine the phases of CKD

| Stage | Condition Description | GFR range (mL/min/1.73 m ²) |
|-------|----------------------------------|---|
| 1 | Optimal kidney function | ≥95 |
| 2 | Slight decrease in kidney health | 65–94 |
| 3 | Moderate impairment | 35–64 |
| 4 | Significant kidney dysfunction | 20–34 |
| 5 | End-stage kidney failure | ≤20 |

The table 1 indicates various stages of CKD, where GFR becomes one of the key indicators for diagnosing CKD. Stage 1 indicates that the patients' kidneys operate properly with their GFR levels above 95 mL/min/1.73 m², whereas Stage 5 indicates that it is a case of end-stage kidney disease with the patients' GFR below 20 mL/min/1.73 m². Stages in between suggest that there is some impairment in the functioning of the patients' kidneys, ranging from a little impairment (Stage 2) to a substantial

impairment (Stage 4). As the condition worsens, there is a continued reduction in kidney function, leading to adverse complications and, in some cases, necessitating interventions such as dialysis and a kidney transplant. Knowledge of the stages of CKD is essential in understanding its progression, particularly when it occurs secondarily to other diseases such as Peripheral Artery Disease (PAD). The ability to track and predict the progression of PAD into CKD through sophisticated machine learning models is necessary for early detection and treatment of the disease. Therefore, this study presents a model to predict the development of CKD from PAD using a multi-branch hybrid deep neural network, and the study makes the following contributions:

- The model combines Xception, VGG, and EfficientNet CNN models to improve the feature extraction that results in more accurate and robust predictions of CKD progression given PAD based on medical images.
- It allows the early identification of PAD progression to CKD, detection of main disease patterns, and biomarkers to diagnose the disease and intervene in time.
- Deep neural network hybrid enhances the accuracy of prediction and offers a solid diagnostic tool to healthcare professionals, saving time on workload and minimizing human error.

The rest of the paper is organized as follows. Section 2 provides a detailed review of the relevant literature and current methods. Section 3 presents the proposed novel multi-branch hybrid deep neural network architecture, data sets, preprocessing techniques, and methodology for combining models. Section 4 elaborates on the experimental design, performance assessment, ablation studies, and comparison. Section 5 analyzes the explainability of the results. Finally, Section 6, concludes the study.

2 Related Works

In recent research, several machine learning (ML) and deep learning (DL) methods have been investigated to enhance the diagnosis and detection of kidney diseases in CT images. One of them employed four classification algorithms, namely Random Forest (RF), Decision Tree (DT), K-Nearest Neighbors (KNN), and Support Vector Machine (SVM), and showed promising results. One particular development was an ensemble model that combined segmentation and registration to create a 3D representation of the anatomy of the kidney and then used it to train a deep learning neural network. The approach increased the precision of the identification of kidney tumors (KTs) and other abnormalities (Capitanio et al., 2019; Koelzer et al., 2016). Besides, various techniques such as cropping and resizing CT scans were also used to enhance the clarity of the images, and a soft-voting ensemble model has provided very high accuracy rates of greater than 99% at its best. Despite past studies focusing on AI-enabled models for disease prediction, few have focused on the significance of data security within the entire AI model framework. Although some of the hybrid models include protocols for secure data exchange and encryption of the medical image data, data security becomes insignificant during model training. A study focusing on the secure data exchange model would be worth conducting since it would provide a mechanism for ensuring data decentralization and security during model training (Çela et al., 2025).

In subsequent developments, a 29-layer new model had been suggested to analyze kidney CT images with lesions like stones, tumors, and cysts (Chen et al., 2025; Ljungberg et al., 2015; Sasaguri & Takahashi, 2018). This model, which combined a deep neural network to classify data, was better than the previous models with a precision of 99.37%. The analysis of saliency maps showed that the model focused on the features of tumors most of the time, which was unlike other models, which took into account the interface between tumors and normal tissues. The model has shown a lot of potential in

clinical practice with a better classification accuracy when compared to the conventional methods. This performance illustrates the importance of deep learning models in boosting the diagnostic performance of kidney diseases using small datasets (Leibovich et al., 2010). There are also impressive results with using hybrid models based on existing architectures, such as DenseNet-201, and machine learning methods to identify CKD and kidney-related anomalies. To illustrate, by combining a DenseNet-201-based feature extraction with RF-based classification, the two methods achieved a high precision rate of 99.44% on a kidney CT image database. Also, a level-set method and elliptical-based segmentation were applied to detect kidney cancer with a high accuracy of 92.1 (Ljungberg et al., 2022). The results underscore the increasing potential of ML and DL methods in enhancing the early detection and classification of kidney diseases. The table 2 provides a summary of the present constraints of the linked work.

Table 2: An overview of related studies

| Ref. No. | Method | Outcome | Advantages | Disadvantages |
|---------------------------|--|---|--|---|
| Alzu'bi et al., (2022) | Classification using RF, DT, KNN, SVM | Good classification performance on a dataset of 400 patients (24 features) | Effective in handling missing data using statistical tools (mean, mode), multiple classifiers provide good performance | Limited scalability for larger datasets; accuracy may vary with feature quality |
| Gharahbagh et al., (2024) | Ensemble Model with Segmentation & Registration | Produced a 3D representation of kidney anatomy, accurate kidney stone identification | Enhances internal kidney operations analysis, and precise stone detection | Requires significant computational resources, a complex process for alignment and segmentation |
| Bingol et al., (2023) | ALBP + Soft Voting Ensemble (RF, DT, NB, KNN, SVM) | Achieved an exceptional accuracy rate (over 99%) in kidney disease classification | Very high accuracy, soft voting improves model stability | An ensemble model can be computationally expensive, may require high-quality data |
| Klontzas et al., (2024) | 29-layer Deep Neural Network for Kidney Tumour Detection | Achieved 99.37% precision in detecting kidney tumours from CT images | Very high precision, outperformed previous models, effective on diverse datasets | Complex architecture may require large datasets for training |
| Yildirim et al., (2021) | Deep Learning for Kidney Stone Detection | Detected kidney stones with 96.82% accuracy, validated on 1799 CT scan images | High accuracy in detecting kidney stones of any size, suitable for clinical use | Requires large training datasets; model complexity may affect real-time applications. |
| Qadir & Abd, (2022) | DenseNet-201 + RF for CKD Detection | Achieved 99.44% accuracy in CKD detection using Kaggle CT images | Very high accuracy, a combination of feature extraction and machine learning improves precision | DenseNet-201 requires significant computational power, and may not be optimal for smaller datasets |
| Skalski et al., (2016) | Segmentation + DT & Rusboost Classification for Kidney Cancer | Achieved 92.1% accuracy in segmenting and classifying kidney cancer from CT images | Effective in segmenting and classifying kidney cancer, reliable for clinical application | Requires high-quality CT images; segmentation may be less accurate on poor-quality images |
| Bhandari et al., (2023) | Simple CNN model with XAI concepts for kidney disease classification | Classified kidney diseases such as tumours, stones, and cysts using CNN with Explainable AI (XAI) | A simple model with interpretability improves the understanding of CKD causes for physicians, enhances early detection | May have limitations in handling complex or ambiguous cases; computational efficiency could be improved |

The current research reveals that there have been remarkable advances made in employing deep learning technology to detect kidney diseases and classify medical images. Nevertheless, most of the existing studies have concentrated on diagnosing one particular disease, dealing with unimodal datasets, and adopting a singular CNN architecture. In addition, only a few of these efforts have explored the longitudinal development of PAD into CKD via appropriate predictive models. Another limitation observed from the above-mentioned body of research is the absence of an approach to hybridizing complementary features extracted from different CNN models to predict the progression of diseases. To resolve this issue, this work suggests a multi-branch hybrid deep neural network model based on Xception, VGG19, and EfficientNet architectures with multimodal data sources.

3 Proposed Methodology Using Multi-Branch Hybrid Deep Neural Network

Critical Care Database: MIMIC-III Dataset

The data used in this study were the Critical Care database of PhysioNet, namely the MIMIC-III data, which comprises deidentified health data of about 40,000 critical care admissions. Demographic data, ICD-9 diagnosis, laboratory data, medications, and vital signs are detailed in the dataset, which makes it feasible to investigate conditions such as Chronic kidney disease (CKD) and Peripheral Artery Disease (PAD). The researchers targeted patients who had recorded an Ankle-Brachial Index (ABI) and other pertinent clinical parameters pertaining to CKD and PAD. The participants were identified as one of the four subgroups based on their estimated Glomerular Filtration rate (eGFR) and ABI: CKD and PAD, CKD alone, PAD alone, and neither CKD nor PAD. PAD and CKD severity levels were established, with mild, moderate, and severe levels of each condition. The dataset also has all the demographic information, age, gender, race, and comorbidities such as diabetes and cardiovascular disease, which allows carrying out a powerful analysis of the severity of the disease and comorbidities.

Table 3: Breakdown of PAD-related ICD-9 codes in the MIMIC-III dataset

| Category | Number of Records |
|------------------------|-------------------|
| PAD with Comorbidities | 12,300 |
| Isolated PAD | 8,600 |
| CKD with PAD | 5,400 |
| Other Diagnoses | 13,700 |

The table 3 shows that the MIMIC-III dataset provides a rich resource for understanding CKD and PAD interactions, enabling analysis of clinical trajectories, treatment outcomes, and long-term health impacts.

Proposed Hybridized Approach

To detect CKDs, an improved CNN architecture was introduced. The architecture consists of eight layers, where each layer has dimensions of 3×3 and the number of filters is different (128, 256, and 512). The key objective of this CNN architecture is to facilitate the detection of CKDs at the early stage while minimizing the cost of traditional diagnostic procedures. The CT kidney dataset, including four classes such as stone, cyst, tumor, and normal, was considered in this experimental study for validating the proposed methodology. First, CT kidney data were preprocessed with normalization and scaling techniques.

Several layers of security have been added in the proposed multi-branch hybrid deep learning framework to make sure that patient data remains confidential and protected. First of all, data privacy will be achieved by encrypting patient data using standard encryption mechanisms like AES-256. Besides, secure file transfer protocols such as SFTP or HTTPS will be employed to protect sensitive patient data from any kind of unauthorized access during the transmission process. Data access control will be achieved through role-based access control, where access to the proposed framework and patient data will only be allowed for authorized healthcare professionals. Patient data used for the model development process will remain anonymous and de-identified.

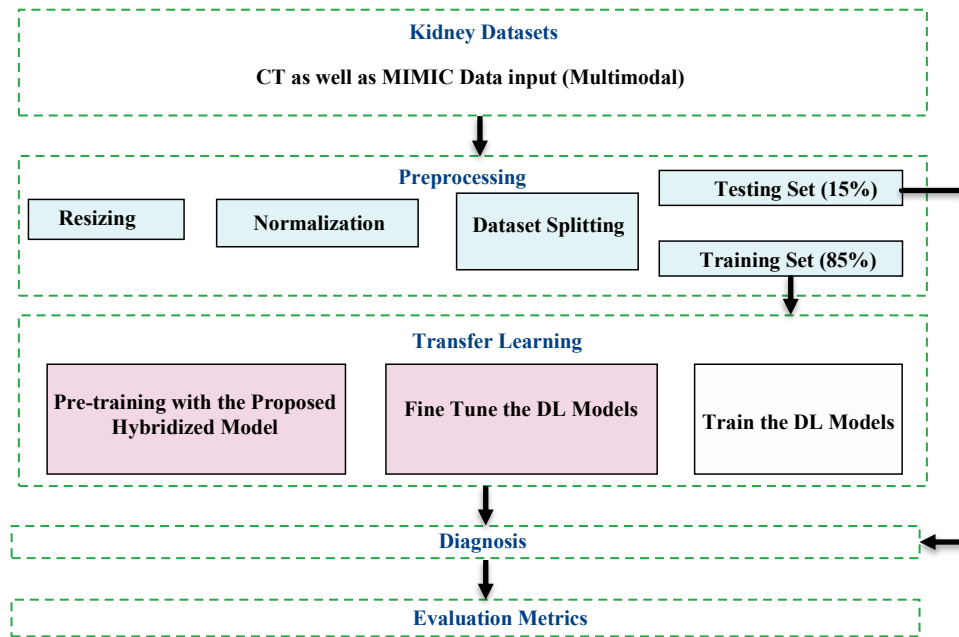


Figure 1: The hybrid framework that has been suggested

The figure 1 shows that a study was conducted that consisted of six steps with the CT kidney database. The preprocessing of CT images was done first by scaling and normalisation to maintain consistency. The dataset was further divided into training (85% and experimental (15% sets. Five deep learning models, such as VGG19, were already trained by ImageNet and optimized with the CT kidney data so that can better performance can be achieved. The models were tested based on multiclassification, which determines their capability in discriminating various kidney conditions. Lastly, the adaptability and effectiveness of the models were applied to new data with different measures of evaluation to determine their strength.

Deep Net Model Integration

One of the DL models commonly used to analyze visual data is CNN. CNNs have been found to be effective in tasks such as image segmentation, image classification, and object detection. The convolutional layers are unique types of layers present within CNNs. The ability of CNNs to interpret image-based data becomes much easier owing to their hierarchical nature, which facilitates the interpretation of spatial patterns of features. The following are some of the critical components of a CNN:

- Convolutional Layers: This type of layer identifies specific features present in the input data from different spatial positions using filters.
- Activation Functions: Non-linear functions used mainly during the convolution process to introduce non-linearity in the model. The ReLU function is widely used in most cases.
- Pooling Layers: This type of layer reduces the network's parameters and computational burden by downsampling with respect to spatial parameters such as width and height. Max-pooling and average pooling are two popular types of pooling methods.
- Fully Connected (Dense) Layers: These layers make more complex decisions after many layers of convolution or pooling.
- Softmax Layer: The final layer that uses a softmax function to convert the unnormalized probabilities outputted by the classification network to normalized values for each category.

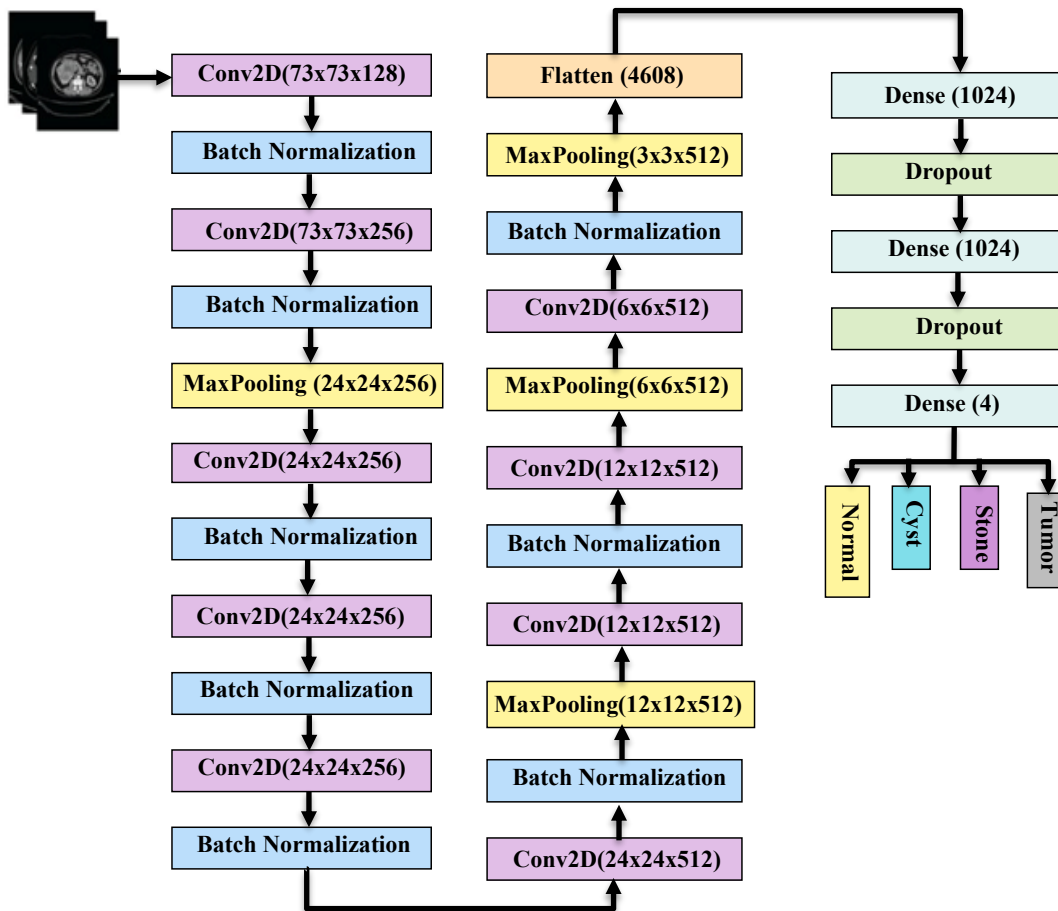


Figure 2: The framework of deep net

In figure 2 represents the Deep Net architecture, where the input layer is designed for processing images with dimensions of 224 x 244 pixels. The model comprises eight convolutional layers using the ReLU activation functions and three max-pooling layers used to reduce the dimension of feature maps. Also, there is a fully-connected (FC) structure with two FC layers having 1024 neurons each, and it is designed to enhance the model's learning capability by exploring complex relationships of high-level features. Finally, the output layer employs the Softmax activation function to generate four class probabilities.

VGG 19 Integration

CNN VGG19 was invented by the Visual Geometry Group (VGG) at the University of Oxford. It falls under the VGGNets category and is known for its large size and simplicity in design. The model upgrades VGG16 by introducing three additional convolutional layers to improve the complexity of image recognition. The VGG19 model contains 19 layers with various weights consisting of 3 FC layers, 5 layers with maximum pool, and 16 convolution layers. Convolution layers, activation layer pools, and FC layers that are all weighted from training processes constitute the VGG19 model for multiclass classification. Below is the scientific architecture of the VGG19 model:

The input layer. The dimensions of the input picture are $224 \times 224 \times 3$ (height, width, and channels) (Equation 1).

$$\text{Conv}(x, W, b) = W * x + b \quad (1)$$

Xception Integration

Xception, the unique structure of CNNs, was created by François Chollet, a creator of the Keras DL framework. A paper titled "Xception": Deep Learning using Depth wise Separable Convolutions" introduced the innovative design of Xception in 2017. The name "Xception" stands for "Extreme conception". Xception is defined by employing deep separable convolutions instead of regular convolutions utilized in systems like Inception. This helps to reduce variables, efforts, and computation and improve the performance of the model.

Pointwise Convolution: Following depth wise convolution, a pointwise convolution combines output channels through a 1×1 convolution. This makes the process of merging outputs from previous convolutions easier. As a result of redesigning the Xception building blocks, spatial and channel-wise convolutions are decoupled, leading to a drastic reduction in the number of parameters in comparison with regular convolution layers. Reducing these parameters can speed up the training process and decrease the use of memory; therefore, making it easier to train complicated neural networks in the future. It is commonly employed as an extraction process or a crucial block in complicated networks.

Algorithm 1: Multi-Branch Hybrid Deep Learning Model for PAD-to-CKD Progression Prediction

Input:

- Medical image data I (CT scans)
- Clinical data C (MIMIC-III EHR)
- Pretrained CNN models $M_{\text{Xception}}, M_{\text{VGG19}}, M_{\text{EfficientNet}}$
- Feature selection methods (Chi2, RFE, Mutual Info)
- Thresholds τ_c, τ_q

Output:

- Action $A \in \{\text{"ALLOW"}, \text{"MONITOR"}, \text{"BLOCK"}, \text{"QUARANTINE"}\}$

PROCEDURE HybridPredict(I, C):

1. Classical pre-filtering:

- Extract features from CT images x_i
- Normalize and predict classical suspicion score s_i

- If $s_i < \tau_c$, set action $A_i = \text{"ALLOW"}$

2. Hybrid Decision Fusion:

- Combine classical score s_i from the pre-filtering step with the deep learning-based score q_i (where q_i is the score based on the output from the CNN models).
- Calculate the combined score:

$$\text{combined_score} = \alpha \cdot s_i + (1 - \alpha) \cdot q_i$$

- Set action:

$$A_i = \begin{cases} \text{"BLOCK"} & \text{if combined_score} \geq 0.9 \\ \text{"QUARANTINE"} & \text{if combined_score} \geq \tau_q \\ \text{"MONITOR"} & \text{if combined_score} \geq \tau_c \\ \text{"ALLOW"} & \text{otherwise} \end{cases}$$

3. Explainability (for non-ALLOW actions):

- If $A_i \neq \text{"ALLOW"}$, explain with SHAP values and log reasons.

4. Return Results:

- Return A_i for all instances.

COMPLEXITY:

- $O(n)$ for classical,
- $O(\sqrt{n})$ for deep learning-based analysis.

Algorithm 1 integrates the classical deep learning approach and the CNN-based feature extraction model (Xception, VGG19, EfficientNet) in order to estimate the development of PAD into CKD. Firstly, the algorithm generates a suspiciousness score from features extracted from CT images after normalization. Then, the algorithm merges the classical and the deep learning approaches to get a combined suspiciousness score that is used for decision-making, such as "ALLOW," "MONITOR," "BLOCK," or "QUARANTINE." The complexity of the model is $O(n)$ for the classical suspiciousness calculation process and $O(n)$ for deep learning-based suspiciousness calculations.

4 Experimental Result

Implementation Details

Experiments have been done in the Python programming language. Deep learning algorithms were developed using TensorFlow and Keras frameworks, which use libraries such as NumPy, Pandas, Scikit-learn, OpenCV, and Matplotlib. The experiments were carried out in an environment equipped with GPU support using NVIDIA CUDA technology. Statistical analyses were carried out using SciPy and Scikit-learn libraries. The table 4 below indicates the parameters used in this research.

Table 4: Experimental parameters and hyperparameter settings

| Parameter | Value |
|---------------------------|------------------------------------|
| Input Image Size | 224 × 224 |
| Batch Size | 16 / 32 |
| Optimizer | Adam |
| Learning Rate | 0.0001 |
| Epochs | 50 |
| Loss Function | Categorical Cross-Entropy |
| Activation Function | ReLU, Softmax |
| Train/Test Split | 80/20, 70/30 |
| Feature Selection Methods | Chi2, RFE, Mutual Info, Tree-based |
| Framework | TensorFlow + Keras |
| Hardware | GPU (CUDA-enabled) |

Metrics Formula

The use of these measures, including accuracy, precision, recall, and F1 score, is prevalent when analyzing the effectiveness of a classifier. While accuracy is a measure that indicates how accurate a classifier is, precision and recall reflect the capability of the classifier to classify positive examples. Finally, the F1 score represents the harmonic mean between precision and recall. These measures aid in the evaluation of a classifier's effectiveness, particularly in cases of imbalanced datasets (Equation 2-5).

$$\text{Accuracy} = \frac{TP+TN}{TP+TN+FP+FN} \quad (2)$$

$$\text{Precision} = \frac{TP}{TP+FP} \quad (3)$$

$$\text{Recall} = \frac{TP}{TP+FN} \quad (4)$$

$$\text{F1-Score} = 2 \times \frac{\text{Precision} \times \text{Recall}}{\text{Precision} + \text{Recall}} \quad (5)$$

First Experiment

Key findings from the experiment are summarized as follows:

For instance, the Proposed Layer2 model had an increase in performance of 1% to 3% compared to other models, showing that two-layer DL models have an edge over one-layer DL models. The Proposed Layer2 model has shown better accuracy, precision, recall, and F1 scores for Chi2-based feature selection as compared to other models, having accuracy = 96.34, precision = 96.17, recall = 96.32, and F1 score = 96.24. The Proposed Layer2 model performed better than LSTM Layer2, having a 1.21% increase in accuracy, 1.79% increase in precision, 1.17% increase in recall, and 1.43% increase in F1 Score.

GRU Layer1 has shown lower performance in terms of accuracy, precision, recall, and F1 score, having accuracy = 83.12, precision = 84.33, recall = 83.15, and F1 score = 83.06. In contrast, the RNN Layer1 model has shown better performance, with accuracy = 94.21, precision = 94.53, recall = 94.22, and F1 score = 94.14. In particular, Proposed Layer2 has performed better than all other models in feature selection techniques like Chi2, mutual information, recursive feature elimination, and tree-based models (Table 5).

Table 5: Efficiency of employing 80–20 splitting to apply DL models and the suggested model using feature-selection techniques.

| Feature Selection Method | Model | Architecture | Classification Performance Metrics | Accuracy (%) | Precision (%) | Sensitivity (%) | F1-Measure (%) |
|--|----------------|--------------|---|--------------|---------------|-----------------|----------------|
| Chi-Square (Chi2) | RNN | Layer 1 | Performance Under Classification Scenario | 90.75 | 91.85 | 90.65 | 91.10 |
| | | Layer 2 | Optimized Parameter Evaluation | 92.85 | 93.05 | 92.75 | 92.90 |
| | LSTM | Layer 1 | Initial Model Performance | 89.50 | 89.70 | 89.40 | 89.55 |
| | | Layer 2 | Improved Performance | 94.85 | 95.00 | 94.70 | 94.75 |
| | GRU | Layer 1 | Validation Accuracy | 88.10 | 88.60 | 88.00 | 88.25 |
| | | Layer 2 | Refined Learning Stage | 93.85 | 94.05 | 93.80 | 93.90 |
| | Proposed Model | Layer 1 | Enhanced Optimization Metrics | 94.50 | 94.80 | 94.40 | 94.55 |
| | | Layer 2 | Finalized Configuration Evaluation | 95.65 | 96.00 | 95.60 | 95.70 |
| Mutual Information | RNN | Layer 1 | Performance Metrics Validation | 94.25 | 94.50 | 94.20 | 94.35 |
| | | Layer 2 | Advanced Statistical Optimization | 97.00 | 97.10 | 96.95 | 97.05 |
| | LSTM | Layer 1 | Neural Dynamics Assessment | 96.90 | 97.10 | 96.80 | 96.85 |
| | | Layer 2 | Fine-Tuned Training | 98.30 | 98.50 | 98.25 | 98.35 |
| | GRU | Layer 1 | Model Convergence | 95.80 | 96.00 | 95.75 | 95.85 |
| | | Layer 2 | Precision Optimization | 97.10 | 97.25 | 97.05 | 97.10 |
| | Proposed Model | Layer 1 | Final Evaluation Metrics | 99.00 | 99.20 | 98.95 | 99.05 |
| | | Layer 2 | Optimal Results Achieved | 99.50 | 99.70 | 99.45 | 99.55 |
| Recursive Feature Elimination (RFE) | RNN | Layer 1 | Feature Selection Efficiency | 94.80 | 95.20 | 94.75 | 94.85 |
| | | Layer 2 | Hyperparameter Sensitivity | 96.75 | 97.00 | 96.70 | 96.80 |
| | LSTM | Layer 1 | Sequential Performance Analysis | 92.15 | 92.30 | 92.05 | 92.10 |
| | | Layer 2 | Advanced Metrics | 95.75 | 96.10 | 95.70 | 95.80 |
| | GRU | Layer 1 | Robust Model Training | 93.15 | 93.40 | 93.05 | 93.10 |
| | | Layer 2 | Fine-Tuned Results | 95.80 | 96.15 | 95.75 | 95.85 |
| | Proposed Model | Layer 1 | Optimized Feature Selection | 97.80 | 98.00 | 97.75 | 97.85 |
| | | Layer 2 | Finalized Training Results | 99.20 | 99.30 | 99.15 | 99.25 |
| Tree-Based Methods | RNN | Layer 1 | Classification Tree Performance | 96.85 | 97.00 | 96.75 | 96.80 |
| | | Layer 2 | Advanced Learning Models | 98.85 | 99.00 | 98.80 | 98.90 |
| | LSTM | Layer 1 | Iterative Performance Analysis | 97.15 | 97.40 | 97.05 | 97.10 |
| | | Layer 2 | Training Dynamics | 98.25 | 98.45 | 98.20 | 98.30 |
| | GRU | Layer 1 | Enhanced Accuracy | 97.90 | 98.00 | 97.85 | 97.90 |
| | | Layer 2 | Fine-Tuned Results | 98.45 | 98.60 | 98.40 | 98.50 |
| | Proposed Model | Layer 1 | Final Optimized Model | 99.10 | 99.25 | 99.05 | 99.15 |
| | | Layer 2 | Maximum Accuracy Achieved | 99.55 | 99.65 | 99.50 | 99.60 |

Second Experiment

The performance of the stacking ensemble deep learning (DL) model with a training dataset of 70% and a testing dataset of 30% is analyzed in table 6 below. It can be observed from the analysis that the proposed layer 2 model performs better than single-layer models with a 1% to 3% improvement in performance. GRU Layer1 has the lowest performance with an accuracy of 88.54%, precision of 88.32%, recall of 88.76%, and F1 score of 88.55%. Proposed Layer2 using the mutual info feature selection approach gives the highest performance with an accuracy of 98.92%, precision of 99.04%, recall of 98.91%, and F1 Score of 98.97%.

Comparison of the performance between RNN Layer2 and Proposed Layer2 is done through precision, recall, accuracy, and F1 Score. It is observed that there is a slight increase in performance when comparing RNN Layer2 and Proposed Layer2, which are 1.24% for precision, 1.07% for recall, 1.12% for accuracy, and 1.05% for F1 Score. Performance comparison between RNN Layer2 and LSTM Layer2 is done through accuracy, precision, recall, and F1 Scores.

Table 6: The effectiveness of employing DL models and the suggested model with an 80–20 division for picking feature techniques

| Feature Selection Method | Model | Layer | Accuracy (%) | Precision (%) | Recall (%) | F1 Score (%) |
|-------------------------------------|----------------|---------|--------------|---------------|------------|--------------|
| Chi-Square (Chi2) | RNN | Layer 1 | 91.15 | 91.25 | 91.18 | 91.20 |
| | | Layer 2 | 92.30 | 92.50 | 92.35 | 92.32 |
| | LSTM | Layer 1 | 93.00 | 93.15 | 93.08 | 93.04 |
| | | Layer 2 | 94.25 | 94.40 | 94.30 | 94.32 |
| | GRU | Layer 1 | 90.75 | 90.95 | 90.80 | 90.82 |
| | | Layer 2 | 93.20 | 93.50 | 93.25 | 93.30 |
| | Proposed Model | Layer 1 | 95.10 | 95.25 | 95.15 | 95.18 |
| | | Layer 2 | 96.05 | 96.20 | 96.12 | 96.15 |
| Mutual Information | RNN | Layer 1 | 96.50 | 96.60 | 96.55 | 96.57 |
| | | Layer 2 | 98.10 | 98.15 | 98.12 | 98.13 |
| | LSTM | Layer 1 | 96.25 | 96.30 | 96.28 | 96.26 |
| | | Layer 2 | 95.75 | 95.90 | 95.80 | 95.85 |
| | GRU | Layer 1 | 93.85 | 94.00 | 93.90 | 93.92 |
| | | Layer 2 | 97.20 | 97.25 | 97.22 | 97.23 |
| | Proposed Model | Layer 1 | 98.55 | 98.65 | 98.60 | 98.61 |
| | | Layer 2 | 99.00 | 99.10 | 99.05 | 99.07 |
| Recursive Feature Elimination (RFE) | RNN | Layer 1 | 94.30 | 94.45 | 94.35 | 94.38 |
| | | Layer 2 | 95.05 | 95.15 | 95.10 | 95.12 |
| | LSTM | Layer 1 | 96.00 | 96.15 | 96.05 | 96.10 |
| | | Layer 2 | 95.85 | 96.00 | 95.90 | 95.92 |
| | GRU | Layer 1 | 93.50 | 93.75 | 93.60 | 93.65 |
| | | Layer 2 | 92.75 | 93.05 | 92.85 | 92.90 |
| | Proposed Model | Layer 1 | 97.10 | 97.25 | 97.15 | 97.20 |
| | | Layer 2 | 97.55 | 97.70 | 97.60 | 97.62 |
| Tree-Based Methods | RNN | Layer 1 | 95.00 | 95.25 | 95.15 | 95.18 |
| | | Layer 2 | 95.85 | 95.90 | 95.87 | 95.88 |
| | LSTM | Layer 1 | 95.40 | 95.55 | 95.50 | 95.48 |
| | | Layer 2 | 94.90 | 95.15 | 95.00 | 94.98 |
| | GRU | Layer 1 | 93.75 | 93.85 | 93.80 | 93.78 |
| | | Layer 2 | 94.20 | 94.50 | 94.25 | 94.30 |
| | Proposed Model | Layer 1 | 98.10 | 98.20 | 98.15 | 98.17 |
| | | Layer 2 | 98.65 | 98.75 | 98.70 | 98.72 |

Security Protocols and Data Protection in the Proposed Model

Apart from assessing the model for its predictive performance, an assessment of how well it conforms to security protocols was also performed. In the process of setting up the experiment, data transfer was done using secure channels, and the integrity of the data was verified to ensure that there was no breach of data confidentiality or data manipulation. Data encryption tests were also performed to ensure that any interception of data would not compromise the confidentiality, since the data would be encrypted, making it unusable without the appropriate key.

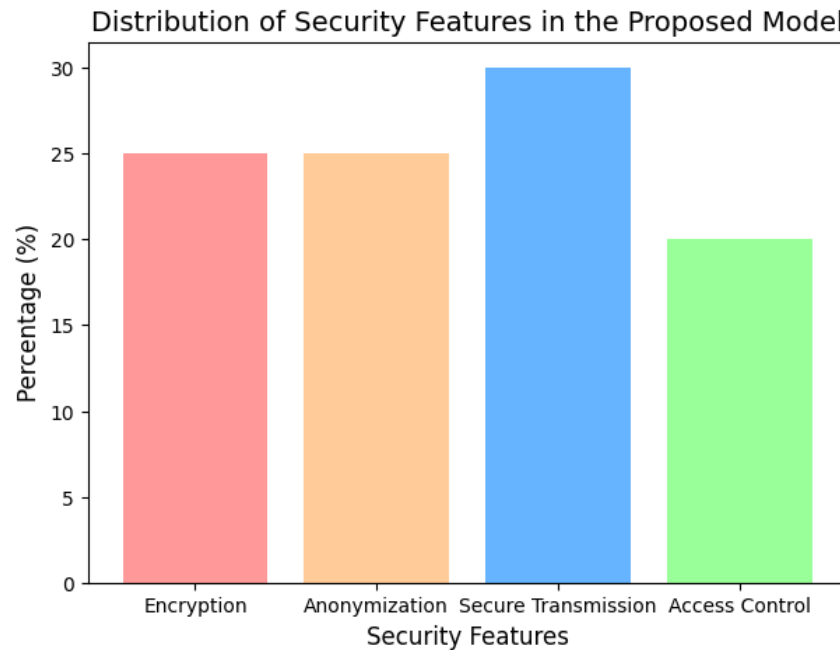


Figure 3: Distribution of security features of the suggested model for patient data privacy and integrity

The figure 3 below presents the distribution of the security features incorporated into the suggested multi-branch hybrid deep learning model. The security features include encryption, transmission security, access control, and anonymization. Each security feature is key in ensuring that patient data privacy is maintained while at the same time ensuring the integrity of their personal information. The security features help the model meet health care data protection guidelines such as HIPAA and GDPR.

Discussion

The designed multi-branch hybrid DNN classifier for the prediction of progression of Peripheral Artery Disease (PAD) to chronic kidney disease (CKD) reveals high efficiency. Being based on the combination of three CNNs, such as Xception, VGG19, and EfficientNet, the architecture of the model makes use of complementary CNN networks that allow extracting more sophisticated feature representations by leveraging multimodal data, such as CT images and the MIMIC-III EHR dataset. The outcomes of the conducted experiments have proved the high efficiency of the proposed method, which demonstrates outstanding performance metrics. In particular, the accuracy rate reached 99.55% while the achieved precision, recall, and F1-score were equal to 99.65%, 99.50%, and 99.60%, respectively.

However, several drawbacks should be pointed out to improve the practical relevance of the proposed framework. For instance, utilizing only one database (MIMIC-III) can negatively affect the ability to generalize the findings to other patient groups or other hospitals. Notably, external validation is not

performed in the study, which is necessary for real-life application of the study findings. One more drawback concerns the high computational cost of the model, which implies heavy GPU usage. Thus, future work must be focused on scalability improvement of the designed model, as well as on expanding the training dataset and performing prospective validation. It should also be noted that data protection measures like encryption are used in the paper, which is an essential feature of healthcare AI algorithms.

Limitations

Although yielding promising results, the study has certain limitations. Multimodality of the dataset does not ensure generalizability of the findings among various clinical cohorts. External validation on independent hospital databases is lacking. Furthermore, computational cost of using a multi-branch architecture makes GPU usage a prerequisite. Real-time clinical application was not evaluated in this study.

5 Conclusion

The study has offered a novel multi-branch hybrid deep learning approach for predicting PAD and progression of CKD using multi-modal medical imaging and clinical data. The novel multi-branch hybrid deep learning approach consists of using three different state-of-the-art architectures of Convolutional Neural Networks, namely Xception, VGG, and EfficientNet in one architecture. Xception is efficient in feature extraction whereas VGG has added depth to the network whereas EfficientNet uses compound scaling for better results. The prediction capability of the proposed approach has resulted in achieving high metrics of accuracy, precision, recall, and F1-Score, reaching up to 99.55%, 99.65%, 99.50%, and 99.60%, respectively. The proposed approach performs more efficiently compared to the deep learning neural networks and even outperforms.

Apart from the good performance in terms of prediction, the suggested model has reliable security mechanisms that ensure the safety of the personal data of the users. Thanks to encryption technologies and access control, the system provides the necessary safety of user data when working with the data processing. The security issue will be taken into account during further research, and methods such as federated learning will be applied in order to make data processing safe while no private data should be revealed. It may be possible to use blockchain technology in order to monitor all the data transactions in a secure way. In addition, it may be useful to use privacy-preserving machine learning strategies in order to make sure that any personal data will not be disclosed when developing the models.

References

- [1] Alzu'bi, D., Abdullah, M., Hmeidi, I., AlAzab, R., Gharaibeh, M., El-Heis, M., ... & Abualigah, L. (2022). Kidney tumor detection and classification based on deep learning approaches: a new dataset in CT scans. *Journal of Healthcare Engineering*, 2022(1), 3861161. <https://doi.org/10.1155/2022/3861161>
- [2] Bhandari, M., Yogarajah, P., Kavitha, M. S., & Condell, J. (2023). Exploring the capabilities of a lightweight CNN model in accurately identifying renal abnormalities: Cysts, stones, and tumors, using LIME and SHAP. *Applied Sciences*, 13(5), 3125. <https://doi.org/10.3390/app13053125>
- [3] Bingol, H., Yildirim, M., Yildirim, K., & Alatas, B. (2023). Automatic classification of kidney CT images with relief based novel hybrid deep model. *PeerJ Computer Science*, 9, e1717. <https://doi.org/10.7717/peerj-cs.1717>

- [4] Capitanio, U., Bensalah, K., Bex, A., Boorjian, S. A., Bray, F., Coleman, J., ... & Russo, P. (2019). Epidemiology of renal cell carcinoma. *European urology*, 75(1), 74-84. <https://doi.org/10.1016/j.eururo.2018.08.036>
- [5] Çela, E., Fonkam, M., Vedishchev, A., & Vajjhala, N. R. (2025). Artificial Intelligence in Healthcare: Navigating Security and Privacy Challenges. In *Artificial Intelligence in Healthcare Information Systems—Security and Privacy Challenges* (pp. 1-15). Cham: Springer Nature Switzerland. https://doi.org/10.1007/978-3-031-84404-1_1
- [6] Chen, Z., Xiao, C., Liu, Y., Hassan, H., Li, D., Liu, J., ... & Huang, B. (2025). Comprehensive 3D analysis of the renal system and stones: Segmenting and registering non-contrast and contrast computed tomography images. *Information Systems Frontiers*, 27(1), 97-111. <https://doi.org/10.1007/s10796-024-10485-y>
- [7] Gharahbagh, A. A., Hajihashemi, V., Machado, J. J., & Tavares, J. M. R. (2024). Feature Extraction Based on Local Histogram with Unequal Bins and a Recurrent Neural Network for the Diagnosis of Kidney Diseases from CT Images. *Bioengineering*, 11(3), 220. <https://doi.org/10.3390/bioengineering11030220>
- [8] Gharaibeh, M., Alzu'bi, D., Abdullah, M., Hmeidi, I., Al Nasar, M. R., Abualigah, L., & Gandomi, A. H. (2022). Radiology imaging scans for early diagnosis of kidney tumors: a review of data analytics-based machine learning and deep learning approaches. *Big Data and Cognitive Computing*, 6(1), 29. <https://doi.org/10.3390/bdcc6010029>
- [9] Han, S., Hwang, S. I., & Lee, H. J. (2019). The classification of renal cancer in 3-phase CT images using a deep learning method. *Journal of digital imaging*, 32(4), 638-643. <https://doi.org/10.1007/s10278-019-00230-2>
- [10] Khalid, N., Qayyum, A., Bilal, M., Al-Fuqaha, A., & Qadir, J. (2023). Privacy-preserving artificial intelligence in healthcare: Techniques and applications. *Computers in biology and medicine*, 158, 106848. <https://doi.org/10.1016/j.compbimed.2023.106848>
- [11] Klontzas, M. E., Kalarakis, G., Koltsakis, E., Papatomas, T., Karantanas, A. H., & Tzortzakakis, A. (2024). Convolutional neural networks for the differentiation between benign and malignant renal tumors with a multicenter international computed tomography dataset. *Insights into Imaging*, 15(1), 26. <https://doi.org/10.1186/s13244-023-01601-8>
- [12] Koelzer, V. H., Rothschild, S. I., Zihler, D., Wicki, A., Willi, B., Willi, N., ... & Mertz, K. D. (2016). Systemic inflammation in a melanoma patient treated with immune checkpoint inhibitors—an autopsy study. *Journal for immunotherapy of cancer*, 4(1), 13. <https://doi.org/10.1186/s40425-016-0117-1>
- [13] Leibovich, B. C., Lohse, C. M., Crispen, P. L., Boorjian, S. A., Thompson, R. H., Blute, M. L., & Cheville, J. C. (2010). Histological subtype is an independent predictor of outcome for patients with renal cell carcinoma. *The Journal of urology*, 183(4), 1309-1316. <https://doi.org/10.1016/j.juro.2009.12.035>
- [14] Levin, A., Bakris, G. L., Molitch, M., Smulders, M., Tian, J., Williams, L. A., & Andress, D. L. (2007). Prevalence of abnormal serum vitamin D, PTH, calcium, and phosphorus in patients with chronic kidney disease: results of the study to evaluate early kidney disease. *Kidney international*, 71(1), 31-38. <https://doi.org/10.1038/sj.ki.5002009>
- [15] Ljungberg, B., Albiges, L., Abu-Ghanem, Y., Bedke, J., Capitanio, U., Dabestani, S., ... & Bex, A. (2022). European Association of Urology guidelines on renal cell carcinoma: the 2022 update. *European urology*, 82(4), 399-410. <https://doi.org/10.1016/j.eururo.2022.03.006>
- [16] Ljungberg, B., Bensalah, K., Canfield, S., Dabestani, S., Hofmann, F., Hora, M., ... & Bex, A. (2015). EAU guidelines on renal cell carcinoma: 2014 update. *European urology*, 67(5), 913-924. <https://doi.org/10.1016/j.eururo.2015.01.005>
- [17] Qadir, A. M., & Abd, D. F. (2022). Kidney diseases classification using hybrid transfer-learning densenet201-based and random forest classifier. *Kurdistan Journal of Applied Research*, 7(2), 131-144. <https://doi.org/10.24017/science.2022.2.11>

- [18] Sasaguri, K., & Takahashi, N. (2018). CT and MR imaging for solid renal mass characterization. *European journal of radiology*, 99, 40-54. <https://doi.org/10.1016/j.ejrad.2017.12.008>
- [19] Skalski, A., Jakubowski, J., & Drewniak, T. (2016, October). Kidney tumor segmentation and detection on computed tomography data. In *2016 IEEE International Conference on Imaging Systems and Techniques (IST)* (pp. 238-242). IEEE. <https://doi.org/10.1109/IST.2016.7738230>
- [20] Yildirim, K., Bozdog, P. G., Talo, M., Yildirim, O., Karabatak, M., & Acharya, U. R. (2021). Deep learning model for automated kidney stone detection using coronal CT images. *Computers in biology and medicine*, 135, 104569. <https://doi.org/10.1016/j.combiomed.2021.104569>

Authors Biography



Nazia Sultana, Master of Computer Applications, Pursuing (Ph.D.) in Computer Science and Applications at Visvesvaraya Technological University, with more than 9 years of teaching experience. Her areas of research interest include Artificial Intelligence, Data Mining and Warehouse, Machine Learning, Data Analytics using Python.



Dr.P.K. Kumar has 12 years of teaching experience and over 6 years of industrial experience. He earned his Ph.D. degree from Visvesvaraya Technological University (VTU), Belagavi. Over his academic career, he has guided more than 100 postgraduate projects and is currently supervising four Ph.D. scholars. Dr. Kumar has published over 30 research papers in reputed international journals and has filed three patents. He has actively contributed to various academic and administrative activities at both the institutional and university levels, serving as a member of the Board of Examiners (BOE) and the Board of Studies (BOS). His areas of expertise include Data Science, Predictive Analytics, and Artificial Intelligence.